Adsorption (2013) 19:143–159
DOI 10.1007/s10450-012-9435-x

Adsorption of ammonia and water on functionalized edge-rich carbon nanofibers

Yusuke Takahashi · Hirotaka Fujita · Akiyoshi Sakoda

Received: 9 November 2011 / Accepted: 29 September 2012 / Published online: 12 October 2012

Abstract The preparation, characterization and ammonia and water adsorption properties of edge-rich carbon nanofibers (CNFs) were studied, including platelet CNFs (PCNFs) and cup-stacked CNFs (CSCNFs). Since PCNFs and CSCNFs have many chemically active exposed edges, functionalization by oxidizing the edges was carried out by ozone stream and by nitric acid. Transmission electron microscopy, N_2 adsorption isotherms and temperature-programmed desorption analysis showed that the nitric acid treatment partly destroyed the graphite structure of the PCNFs and created acid functional groups and micropores, whereas the ozone treatment created functional groups without damaging the structure. Ammonia adsorption isotherms clarified that NH_3 adsorption on PCNFs and CSCNFs occurred mainly on oxygen-containing groups, whereas the adsorption on activated carbon fibers (ACFs) occurred on both oxygen-containing groups and the carbon surface without the functional groups, and the CSCNFs showed larger amounts of adsorbed ammonia compared to the PCNFs. Especially at a relatively low pressure range (<0.2 atm), the PCNFs/CSCNFs/ACFs showed the same ammonia adsorption mechanism; that is, the one-to-one interaction between oxygen atoms in the functional groups and hydrogen atoms in ammonia molecules. In addition, the adsorption on the ACFs appeared to occur mainly by interaction with the carbon surface at relatively high pressure (0.3–1.0 atm). Our experimental results and previous findings suggest that NH_3 adsorption on PCNFs is due mainly to NH...O hydrogen bonding between oxygen-containing groups and ammonia rather than to chemical bonding.

Y. Takahashi (✉) · H. Fujita · A. Sakoda
Institute of Industrial Science, University of Tokyo,
4-6-1 Komaba, Meguro-ku, Tokyo 153-8505, Japan
e-mail: ekusu@iis.u-tokyo.ac.jp

Keywords Carbon nanofiber · Adsorption · Ammonia · Water

1 Introduction

Carbon nanotubes/nanofibers (CNTs/CNFs) have attracted many researchers' attention due to their unique physical and chemical properties that indicate potential applications in fuel cells, adsorbents, chemical sensors and so on (Endo et al. 2006a, 2006b). Many authors have already reported on the adsorption properties and chemical sensor performance of functionalized CNTs (Kong et al. 2000; Wang 2005; Sinha et al. 2006; Peng et al. 2009), but there have been few studies on the adsorption properties of CNFs in comparison to CNTs.

CNFs are categorized into the following four types, based primarily on the graphene layer alignment with respect to the fiber axis and whether the fiber has a hollow core: (1) platelet type (PCNFs), in which the graphene layers are aligned at right angles to the fiber axis (Baker 1989), (2) herring-bone type (HBCNFs), in which the graphene layers tilt at an angle with respect to the fiber axis, (3) tubular type (TCNFs), in which the graphene layers are parallel to the fiber axis, and (4) cup-stacked type (CSCNFs), in which the graphene layers tilt, like the herring-bone type, but with a different core structure (Yanagisawa et al. 2002). The TCNFs and CSCNFs have hollow cores, whereas the PCNFs and HBCNFs are solid.

Among the types of CNFs, the PCNFs, HBCNFs and CSCNFs have many chemically active exposed edges, indicating a variety of potential applications as catalysts and adsorbents, whereas CNTs and TCNFs have good physical and electrical properties. To date, there has been less research on applications of edge-rich CNFs such as PCNFs and CSCNFs

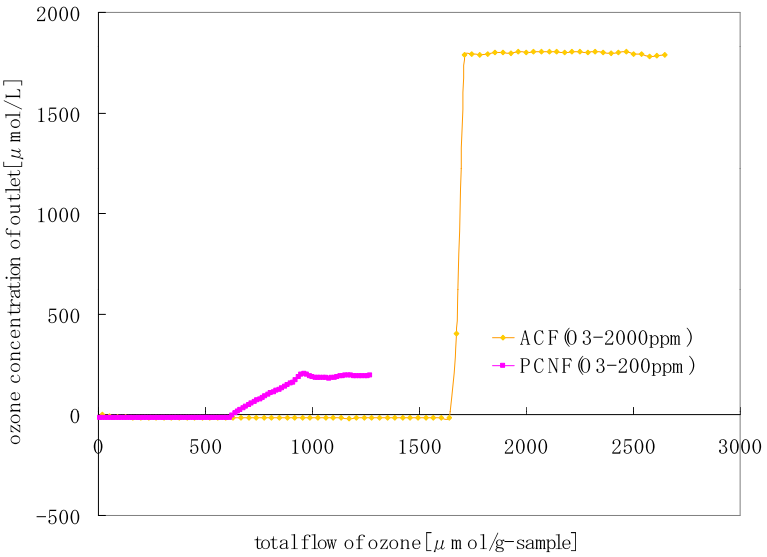

Fig. 1 Breakthrough curve for ozone treatment

as adsorbents or chemical sensors compared to the research on CNTs and TCNFs.

Regarding CNT applications as gas sensors, the addition of functional groups on the CNT surface improved gas sensing performance (Chang et al. 2001; Wu et al. 2007), in which the sensing mechanism is said to be a charge transfer caused by gas adsorption to functional groups added on the CNT surface. Functionalized CNFs appear to have potential applications as adsorbents, and, considering the abundant exposed edges on CNFs, functionalization should markedly improve the adsorption performance. CNF functionalization is required to prevent the destructuring of CNFs, since various potential applications involving catalysts support (Bessel et al. 2001), polymer composites (Amorim et al. 2005; Tibbetts et al. 2007) and sensing devices (Melechko et al. 2005; Peng et al. 2009) require their unique structure and characteristics.

This work had two objectives. The first was to evaluate the performance of PCNFs and CSCNFs as adsorbents, to test our hypothesis that the functionalization of the large number of active edges on the edge-rich CNF surface would improve and control the adsorption properties. With the exception of an N_2 adsorption isotherm analysis, no detailed study of CNF adsorption performance has been reported to date, to the best of our knowledge. The second objective was to discuss the mechanism of ammonia adsorption and the relationship between functional groups and adsorption equilibria. There have been various reports about ammonia adsorption on CNTs. For example, a binding energy calculation of ammonia adsorption clarified that ammonia adsorption on metallic CNTs is slightly stronger than that on semi-conducting CNTs, and that when the CNTs diameter increased, the binding energy decreased (Lu et al. 2005; Shirvani et al. 2010). It was also shown that the conductivity change of CNTs by ammonia adsorption was derived from electron charge transfer (Chang et al. 2001). In addition, experimental ammonia adsorption on CNTs has shown that the amount of ammonia adsorption is sensitive to functionalities and defect sites on the CNT surface (Feng et al. 2005). However, most studies have focused on the electrical characteristics of CNTs and their application in chemical sensors, with few studies of the adsorption isotherm or adsorptive capacity. Also, few studies of the relationship between functional groups and adsorption properties of CNTs/CNFs have been reported.

2 Experiments

2.1 PCNF samples

In this work we used three carbon materials: (1) PCNFs (commercial name: PGNF [platelet graphite nanofiber] purchased from Catalytic Materials, Holliston, MA, USA). (2) CSCNFs prepared by the poly(ethylene glycol) (PEG)-pyrolysis method as described in our previous research (Takahashi et al. 2010). PEG was added to the aqueous solution of $NiCl_2$, and the mixed solution was uniformly spread on a silicon wafer, followed by drying on a hot plate. Subsequently, the mixture on the silicon wafer was placed in a tubular furnace and heated to 750 °C for the growth of CNFs. (3) Activated carbon fibers (ACFs) (commercial name: A-15) purchased from Osaka Gas (Osaka, Japan), for comparison with the PCNFs and CSCNFs.

In one type of pretreatment, samples of each type of carbon material were packed in glass columns (diameter: 1 cm) and connected to an ozone generator (POX-10, Fuji Electric, Tokyo, Japan) to oxidize the carbon materials with a 500–10000 ppm ozone stream for more than 4 hr until the

output concentration of the ozone was saturated. The breakthrough curves for some of the experiments are shown in Fig. 1. We called the samples "PCNF–O_3," "CSCNF–O_3," and "ACF–O_3."

In another type of pretreatment, 300-mg samples of each type of carbon material were sintered in 100 mL HNO_3 (Wako Chemicals, Osaka, Japan) with the concentration ranging from 1.3 N to 13 N, and stirred at 400 rpm for 2 hr at 373 K in an oil bath. Next, each sample was suction-filtered and rinsed by distilled water four times, and then dried in an oven at 333 K for 10 hr. We called these samples "PCNF–HNO_3," "CSCNF–HNO_3," and "ACF–HNO_3."

As a third type of pretreatment, as-prepared (that is, non-oxidized) materials were placed in a tubular furnace and heated at 1273 K for 2 hr in a 500 mL/min N_2 flow to remove the functional groups on the carbon surface. We called these samples "PCNF–N_2," "CSCNF–N_2," and "ACF–N_2." The purpose of this sample was to allow us to distinguish the effect of functional groups on NH_3 adsorption from that of micropores. In this study, the external and internal structures of the above-mentioned samples were investigated by scanning electron microscopy (SEM) and transmission electron microscopy (TEM).

2.2 TPD analysis

The changes in surface functional groups on each sample were measured by temperature programmed desorption (TPD). TPD analysis is a well-established method for characterizing the functional groups on carbon materials such as CNFs (Rosenthal et al. 2010), CNTs (Delhaes et al. 2006) and activated carbon (Figueiredo et al. 1999). In this experiment, 200 mg of each sample was put on a ceramic boat and placed in a quartz tube. The boat containing the sample was heated from the ambient temperature to 1273 K under an N_2 flow (800 mL/min) to decompose the oxygen-containing surface functional groups to CO/CO_2 gas by an electrical furnace, where the ramping rate was 5 K/min. The N_2 flow was controlled by a mass flow controller (model 3660, Kofloc, Kyoto, Japan), and the desorbed gases from the samples were measured with a CO/CO_2 concentration meter (HT-1210N, Hodaka Co., ltd., Osaka, Japan and ZFP5YA31, Fuji Electric, Tokyo, Japan).

2.3 Adsorption isotherms of nitrogen, ammonia and water

Nitrogen isotherms on each sample were measured with a Belsorp 36 (Bell Japan, Osaka, Japan) to estimate the specific surface area by the BET method (defining the Brunauer, Emmet and Teller [BET] surface area) and the porosity by the t-plot method.

An ammonia isotherm was measured with a gravimetric adsorption apparatus. In this study, ammonia was used as a main adsorbate, because NH_3 is a basic gas that interacts with oxygen-containing functional groups, and it was thus expected to show good adsorption performance to functionalized PCNFs and CSCNFs as well as activated carbon (Tamon and Okazaki 1996; Park and Kim 1999; Park and Jin 2005; Huang et al. 2008; Shan et al. 2008; Ko et al. 2012).

First, each carbon sample was placed in a sample container. Prior to contact with the adsorbate (NH_3), the sample was thoroughly outgassed by evacuation and the initial weight was determined at 300 K. Then, the adsorbate was introduced into the glass chamber containing a PCNF sample, and the pressure was raised from 0 to 1 atm. After equilibrium was achieved, pressure and weight gain (i.e., amount adsorbed) were measured, and the sample was re-degassed at 298 K until a constant weight was again achieved. In addition, water adsorption isotherms were measured on ozone-treated PCNFs and ACFs. H_2O molecules had stronger interaction with oxygen-containing functional groups and were expected to show better adsorption performance than ammonia.

3 Results and discussion

3.1 SEM and TEM observations

SEM and TEM images of PCNFs and CSCNFs are shown in Figs. 2 and 3. As confirmed by the SEM images, the PCNF dia. was 100–300 nm (the mean dia. was approx. 200 nm, except for the carbon nanoparticles [50–200 nm dia.] which the PCNF sample contained) and the length was 1–5 μm. No apparent difference between the as-prepared PCNF samples and the oxidized samples was observed in the SEM images.

The TEM images showed that the PCNFs have a graphite structure perpendicular to the fiber axis and that the PCNF–O_3 maintained its structure, whereas the PCNF–HNO_3 and CSCNF–HNO_3 structure was broken, mainly at the tip of the fiber (Fig. 4). The BET surface area of the PCNFs was increased, which is discussed later regarding nitrogen adsorption isotherms. That result indicated that HNO_3 treatment destructed the graphite structure of the PCNFs and CSCNFs. Similarly, past studies have shown that acid treatment such as nitric acid and sulfuric acid could improve the crystallinity of multi-walled CNTs due to purification, but too much acid treatment broke the graphite layer and loaded the defect site of multi-walled CNTs (Wang et al. 2003; Kim et al. 2008; Yang et al. 2008). Therefore, ozone treatment might be useful compared to nitric acid treatment, since PCNF functionalization without the graphite destructuring has more potential applications (Bessel et al. 2001; Tibbetts et al. 2007; Amorim et al. 2005; Melechko et al. 2005; Peng et al. 2009).

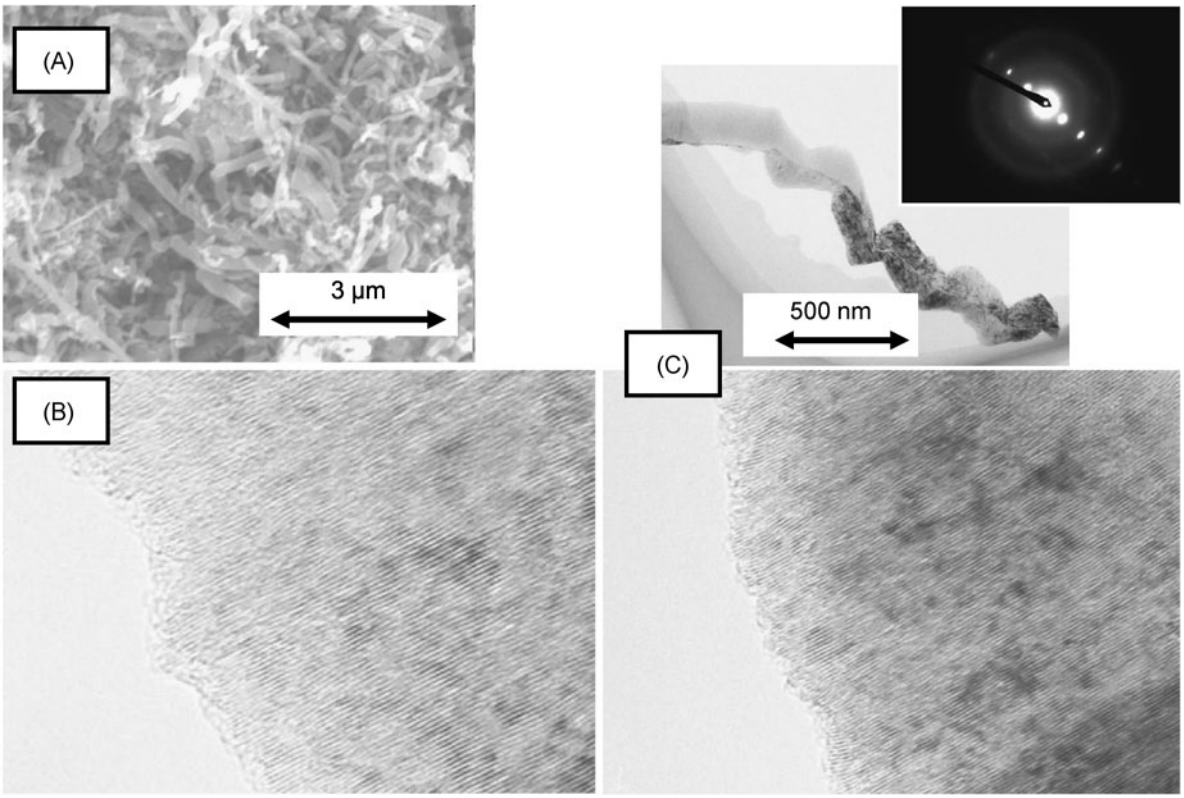

Fig. 2 SEM images of (**A**) PCNF, and TEM images of (**B**) PCNF and (**C**) PCNF–O_3 (10000 ppm). The *insert* in (**C**) is the SAED pattern of PCNF–O_3

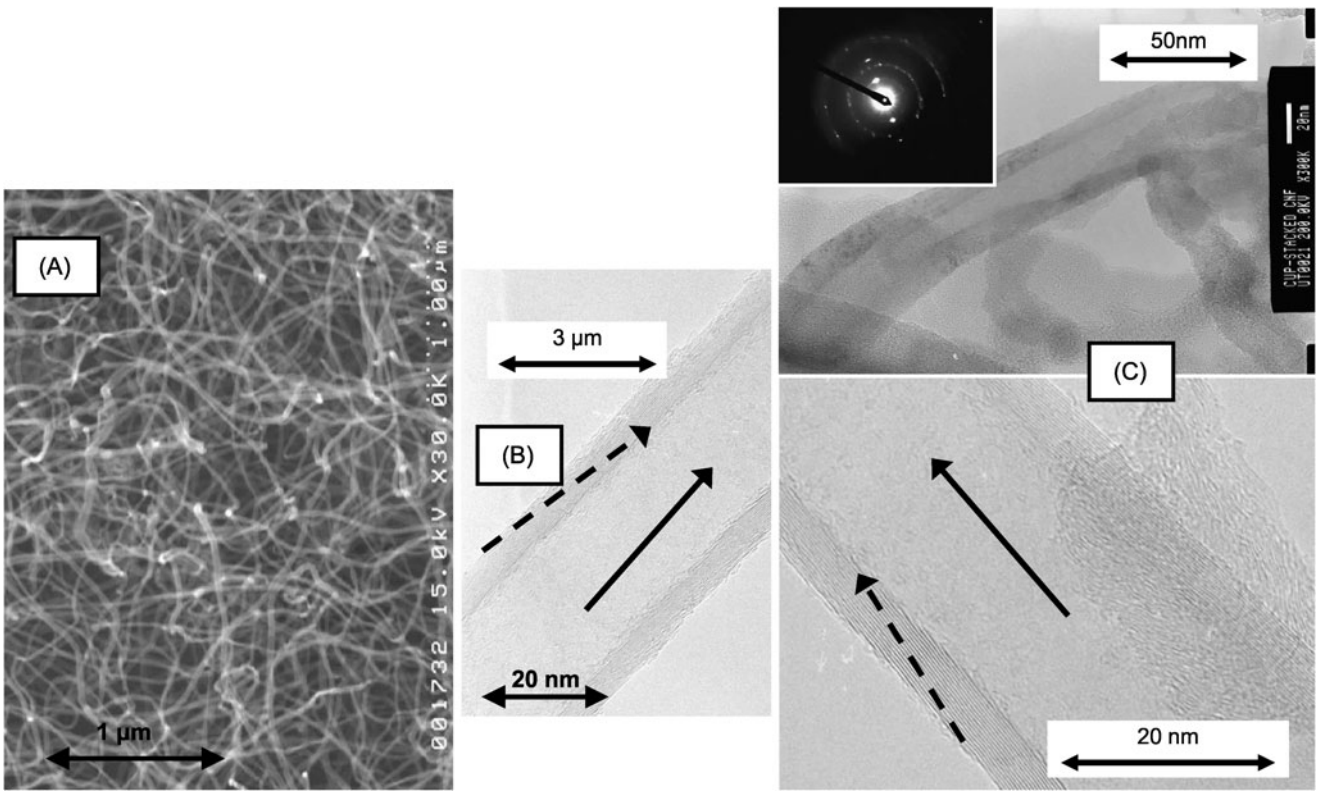

Fig. 3 SEM images of (**A**) CSCNF, and TEM images of (**B**) CSCNF and (**C**) CSCNF–O_3 (10000 ppm). The *insert* in (**C**) is the SAED pattern of CSCNF–O_3

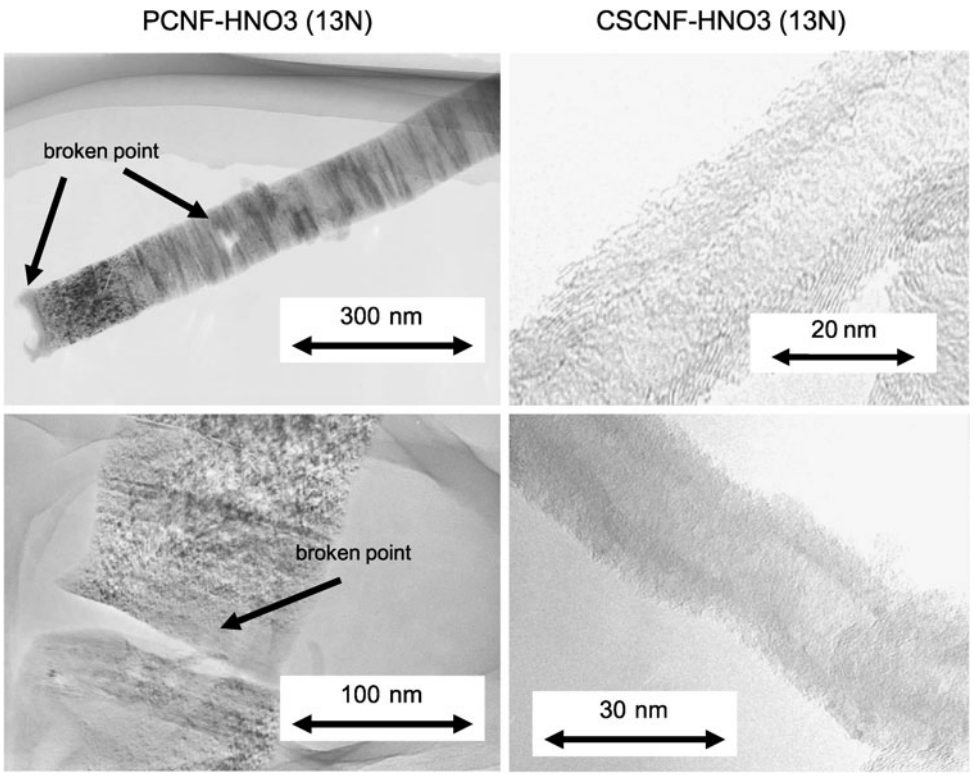

Fig. 4 PCNF and CSCNF oxidized by HNO_3 (13 N)

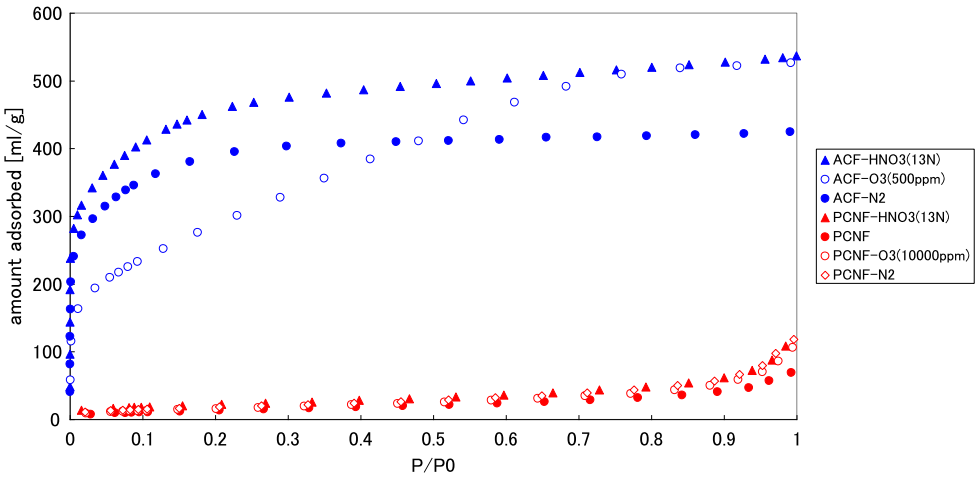

Fig. 5 N_2 isotherm of PCNF/ACF

Table 1 BET surface area and micropore analysis by DR plot for PCNF and ACF

	BET constant (C)	BET surface area [m^2/g]	Micropore surface area [m^2/g]	Micropore volume W_0 [cc-gas/g]	W_0/W_{sat} [–]
PCNF–HNO_3(13 N)	133	76.9	18.2	23.1	0.213
PCNF–O_3(10000 ppm)	55.4	59.5	16.1	17.11	0.160
PCNF–N_2	64.8	66.7	17.2	17.9	0.152
ACF–N_2	344	1238	1056	323	0.763
ACF–O^3	82.1	1038	957	255	0.484
ACF–HNO^3	326	1724	1689	779	0.690

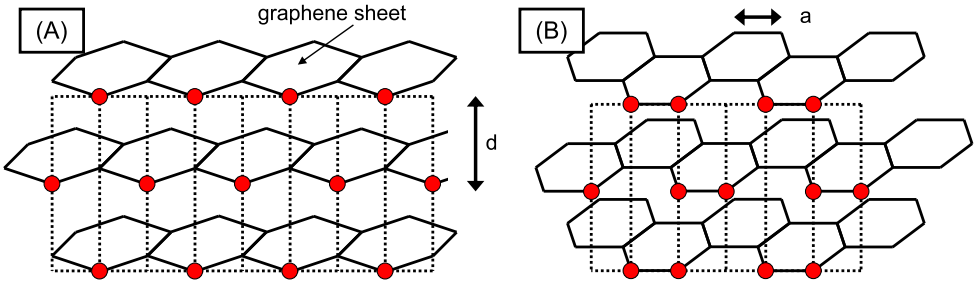

Fig. 6 Schematic diagrams of two types of edge surface of PCNF/CSCNF. (**A**) Zigzag edge; (**B**) armchair edge

3.2 BET surface area and micropore volume

The analysis results of the nitrogen adsorption isotherm are shown in Fig. 5 and Table 1. The analysis confirmed that PCNFs have a very small BET surface area (51.4 m^2/g) and much less pore volume compared to activated carbon (Guo et al. 2005) and ACFs, as shown in Table 1. It was reported that ozonization decreased the BET surface area and micropore volume for activated carbon (Rivera-Utrilla et al. 2011). This may have been because the acid functional groups on the PCNF surface disturbed nitrogen adsorption. In addition, the analysis of the PCNF–N_2 showed that HNO_3 treatment followed by heat treatment increased the BET surface area and micropore volume compared to those of the PCNFs. In a previous study the surface area did not change so much, and the acid functional groups of CNTs were reduced by heating in an inert gas atmosphere at 973 K (Byl et al. 2005). This finding led us to suspect that the surface area difference between as-prepared PCNFs and PCNF–N_2 was caused mostly by the decomposition of surface functional groups, not by a structural change of PCNF.

3.3 Functional groups

Prior to the TPD analysis conducted to evaluate the amount of oxygen-containing functional groups on the CNF/ACF surface, we estimated the amount of CNF exposed edges based on an idealized edge surface morphology, as shown in Fig. 6. For the calculations, the following were assumed:

- The CNF edge surface consists of a zigzag or an armchair edge, as illustrated in previous work about graphite characteristics (Hemraj-Benny et al. 2008).
- The surface area of the basal plane on CNFs is very small and can be ignored compared to the edge surface.
- The surface area containing exposed edges is measured as a flat surface, as shown in the dotted line region in Fig. 5.
- The CNF density and the shape of six-membered rings forming graphene sheets in CNF are the same as those of graphite.
- All of the exposed edges (as shown in Fig. 5) are chemically active.

As a result of these assumptions, we calculated the surface area on the CNF edge surface [nm^2] illustrated as the dotted line region in Fig. 6 as follows, according to the edge state (i.e., zigzag edge or armchair edge):

$$S_{(zigzag\ edge)} = 4\sqrt{3} \times a \times d \times 2 \tag{1}$$

$$S_{(armchair\ edge)} = 6 \times a \times d \times 2 \tag{2}$$

We then calculated the amount of edge per surface area E [$\mu mol/m^2$], as follows:

$$E_{(zigzag\ edge)} = \frac{8 \times 10^{24}}{8\sqrt{3} a d \rho N_A} \tag{3}$$

$$E_{(armchair\ edge)} = \frac{8 \times 10^{24}}{12 a d \rho N_A} \tag{4}$$

where a is the length of a six-membered ring in graphene sheets [nm], d is the distance between graphene sheets [nm], ρ is the density of CNF [g/nm^3], and N_A is the Avogadro constant [mol^{-1}].

Based on past studies of PCNFs, $d = 0.34$ nm (Niimi et al. 2005; Anderson 2006). Here, $\rho = 2.2 \times 10^{-21}$ g/nm^3 and $a = 0.142$ nm from the assumptions described above. Therefore, when the CNF surface consists of a zigzag edge, the theoretical amount of exposed edges per BET surface area was calculated to be 19.85 $\mu mol/m^2$ (12.0 sites/nm^2) from Eq. (3), where it was calculated to be 22.93 $\mu mol/m^2$ (13.8 sites/nm^2) in the case of an armchair edge from Eq. (4).

The results of the TPD analysis of the PCNF, CSCNF and ACF samples are shown in Fig. 7 and Table 2, including the results of our previous work on CSCNF (Ko et al. 2012). From the CO/CO_2 evolution curves, it was confirmed that both ozone and nitric acid oxidation added acid functional groups on the surface of the PCNFs, CSCNFs and ACFs. In the TPD spectra of oxidized samples by O_3, highly intense CO evolutions were mainly observed at 600–650 °C and CO_2 evolutions were observed at around 200 °C. In the case of samples oxidized by HNO_3, CO evolutions were observed at around 700 °C and CO_2 evolutions were observed at 350–400 °C. In the literature, a CO peak around 700 °C was attributed to ether (Aksoylu et al. 2001) or carbonyl (Marchon et al. 1988) decomposition, a CO_2 peak at 100–400 °C was assigned to carboxylic acid

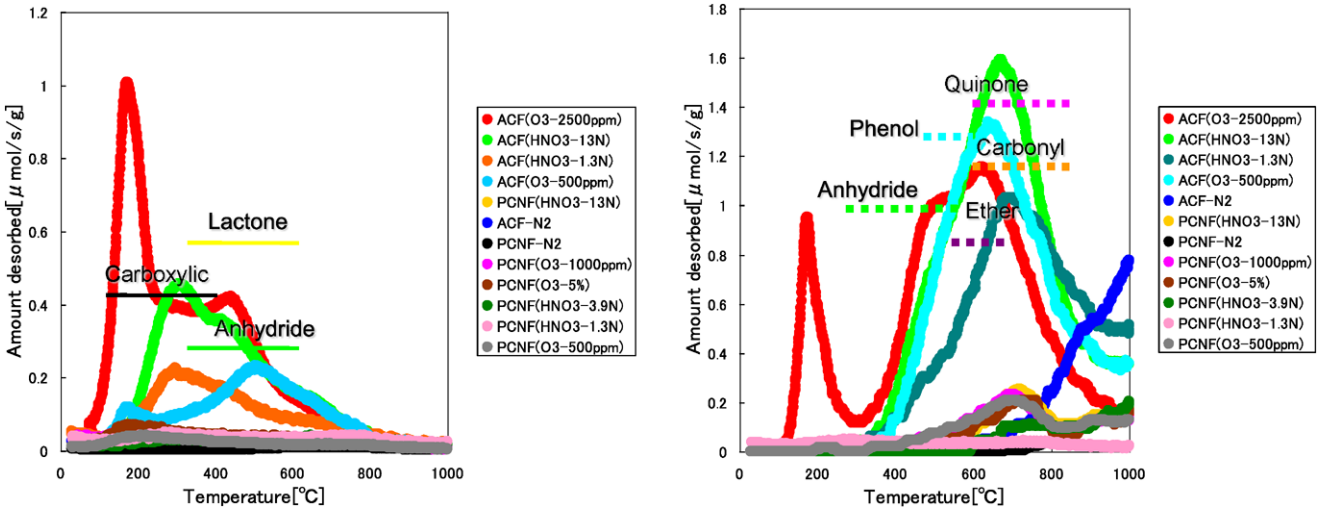

Fig. 7 TPD profile of PCNF and ACF: (*left*) CO_2 evolution, (*right*) CO evolution

Table 2 Amounts of CO and CO_2 released, as obtained by integration of the areas under the TPD peaks of PCNF, CSCNF and ACF before and after different oxidative treatments

	CO_2	CO	Total [μmol/g]
PCNF–N_2-1000 °C	61.1	284	345
PCNF–HNO_3-1.3 N	381	674	1056
PCNF–HNO_3-3.9 N	309	499	808
PCNF–HNO_3-13 N	260	845	1104
PCNF–O_3-500 ppm	233	890	1122
PCNF–O_3-1000 ppm	350	871	1221
PCNF–O_3-10000 ppm	417	757	1174
CSCNF (pristine)*	191	455	645
CSCNF–O_3-1000 ppm*	346	2253	2599
ACF–N_2-1000	324	1487	1811
ACF–HNO_3-1.3 N	1054	4638	5692
ACF–HNO_3-3.9 N	1345	5128	6473
ACF–HNO_3-13 N	1890	6257	8147
ACF–O_3-500 ppm	1113	5459	6572
ACF–O_3-2500 ppm	2400	5573	7974
ACF–O_3-2500 ppm	2486	5481	7968

* Ko S., Takahashi Y., Fujita H., Tatsuma T., Sakoda A., and Komori K.: Peroxidase-Modified Cup-stacked Carbon Nanofiber Networks for Electrochemical Biosensing with Adjustable Dynamic Range. RSC Advances 2, 1444–1449 (2012)

(Zhuang et al. 1994a), and a CO_2 peak at a higher temperature (350–600 °C) was reportedly derived from lactone or anhydride (Zhuang et al. 1994b). Therefore, the CO/CO_2 evolution curve derived in this study indicates that ozone and nitric acid add partly different functional groups on the PCNF/CSCNF/ACF surface. Overall, ozone oxidation adds more carboxyl/phenol groups and fewer anhydride/carbonyl groups to the carbon surface than does nitric acid, which was supported by the previous reports about CNF functionality analysis by TPD/XPS (Rosenthal et al. 2010).

Figure 8 shows the effect of HNO_3/O_3 concentration on the amount of surface functional groups analyzed by TPD for the PCNFs, CSCNFs and ACFs. The PCNFs and CSCNFs showed little difference with regard to the amount of surface functional groups by the concentration of HNO_3 or O_3, which indicated that a relatively mild oxidizing method is sufficient to add functional groups on the PCNF/CSCNF surface to the limit, whereas the functional groups of the ACFs increased according to the concentration of HNO_3 and O_3. Considering the results shown in Fig. 8 and those of previous studies of the oxidation of activated carbon (Zhao et al. 2005; Chen et al. 2007), we conclude that in the present study the PCNF/CSCNF/ACF could be oxidized and functional groups could be added to the limit by HNO_3 or O_3. In one study, the amount of functional groups added to activated carbon by HNO_3 oxidation almost reached a limit when the concentration was 5.4 N, the temperature was 100 °C, and the oxidizing time was 1 h (Zhao et al. 2005).

As shown in Fig. 8 and Table 2, the total CO/CO_2 amounts desorbed were larger in the case of the ACFs than in those of the PCNFs/CSCNFs. This is probably because of the large surface area and small crystal size of ACFs compared to CNFs (Yoon et al. 2004; Zhang et al. 2006; Lee et al. 2007). However, the functional group density per unit of the ACF BET surface area is much smaller than that of the oxidized PCNFs/CSCNFs (Table 3). These results are consistent with previous studies of activated carbon (Afuilar et al. 2003). Even though the BET surface area of activated carbon is likely to be overestimated, this result may indicate that PCNFs and CSCNFs can support functional groups with much higher surface density compared to activated carbon, which indicates their good potential application as adsorbents (Ren et al. 2011).

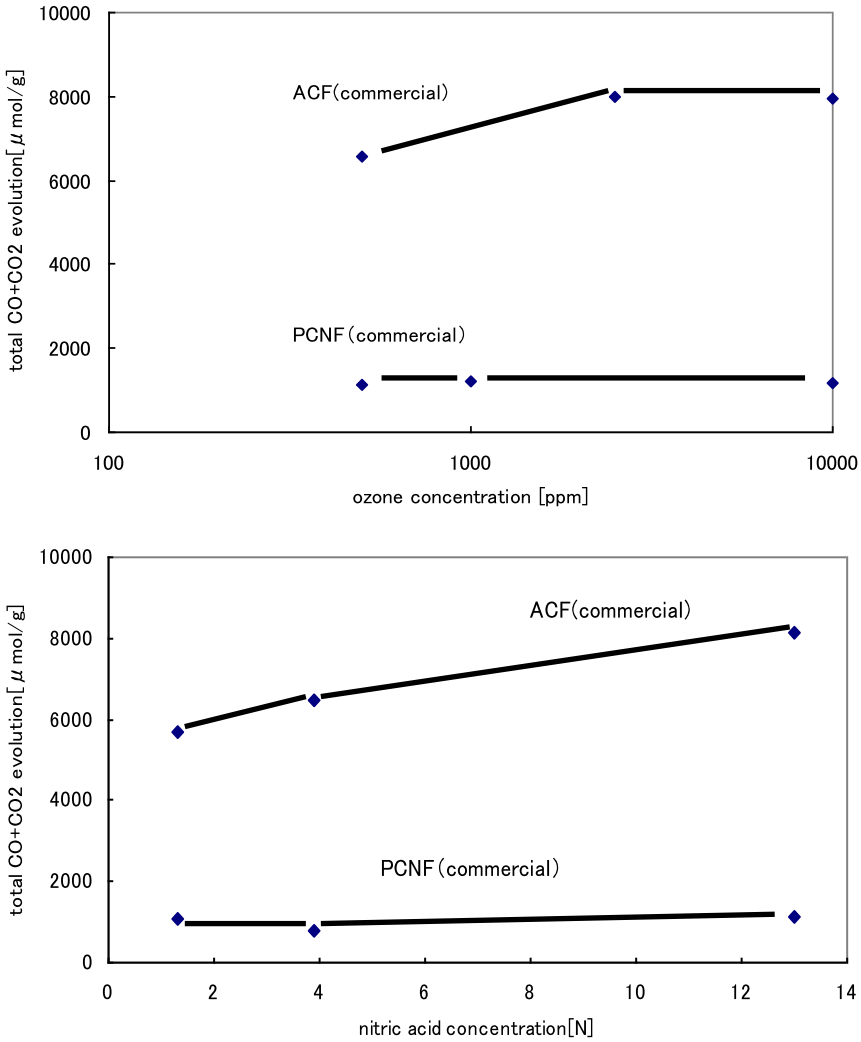

Fig. 8 Effects of HNO_3/O_3 concentration on surface functional groups analyzed by TPD for PCNF/CSCNF/ACF

Table 3 BET total amount of oxygen-containing functional groups per BET surface area

	Total functional group [μmol/g]	BET [m^2/g]	Total functionality per BET [μmol/m^2]
PCNF (N_2)	345	66.7	6.72
PCNF–O_3 (10000 ppm)	1221	66.7	18.3
PCNF–HNO_3 (13 N)	1104	59.5	18.6
CSCNF (pristine)*	645	230	2.80
CSCNF-O_3 (1000 ppm)*	2599	185	14.0
ACF(N_2)	1811	1238	1.46
ACF–O_3 (500 ppm)	6572	1038	6.33
ACF–HNO_3 (13 N)	8147	1724	4.73

*Ko S., Takahashi Y., Fujita H., Tatsuma T., Sakoda A., and Komori K.: Peroxidase-Modified Cup-stacked Carbon Nanofiber Networks for Electrochemical Biosensing with Adjustable Dynamic Range. RSC Advances 2, 1444–1449 (2012)

In the case of PCNF–HNO_3 or –O_3, the total amount of CO/CO_2 evolution per BET surface area reached about 18 μmol/m^2 at maximum, possibly because the graphene layer of the PCNFs was stacked perpendicular to the fiber axis and thus possesses abundant edges per surface area compared to CSCNFs. The reasons why the value could not reach the idealized value (19.85–22.93 μmol/m^2) were probably the structural difference between the idealized graphite edge surface and the actual CSCNF/PCNF surface, and the possibility that some of the exposed edges on the PCNFs/CSCNFs could not support oxygen-containing functional groups because of steric hindrance. However, the test clarified that oxidized PCNFs/CSCNFs were densely functionalized carbon materials with little exposed carbon surface, since functional groups could be added to them much more densely per BET surface area than they could to conventional carbon material such as ACFs. Therefore, functionalized edge-rich CNFs are a unique functional group carrier expected to have unique characteristics as novel adsorbents.

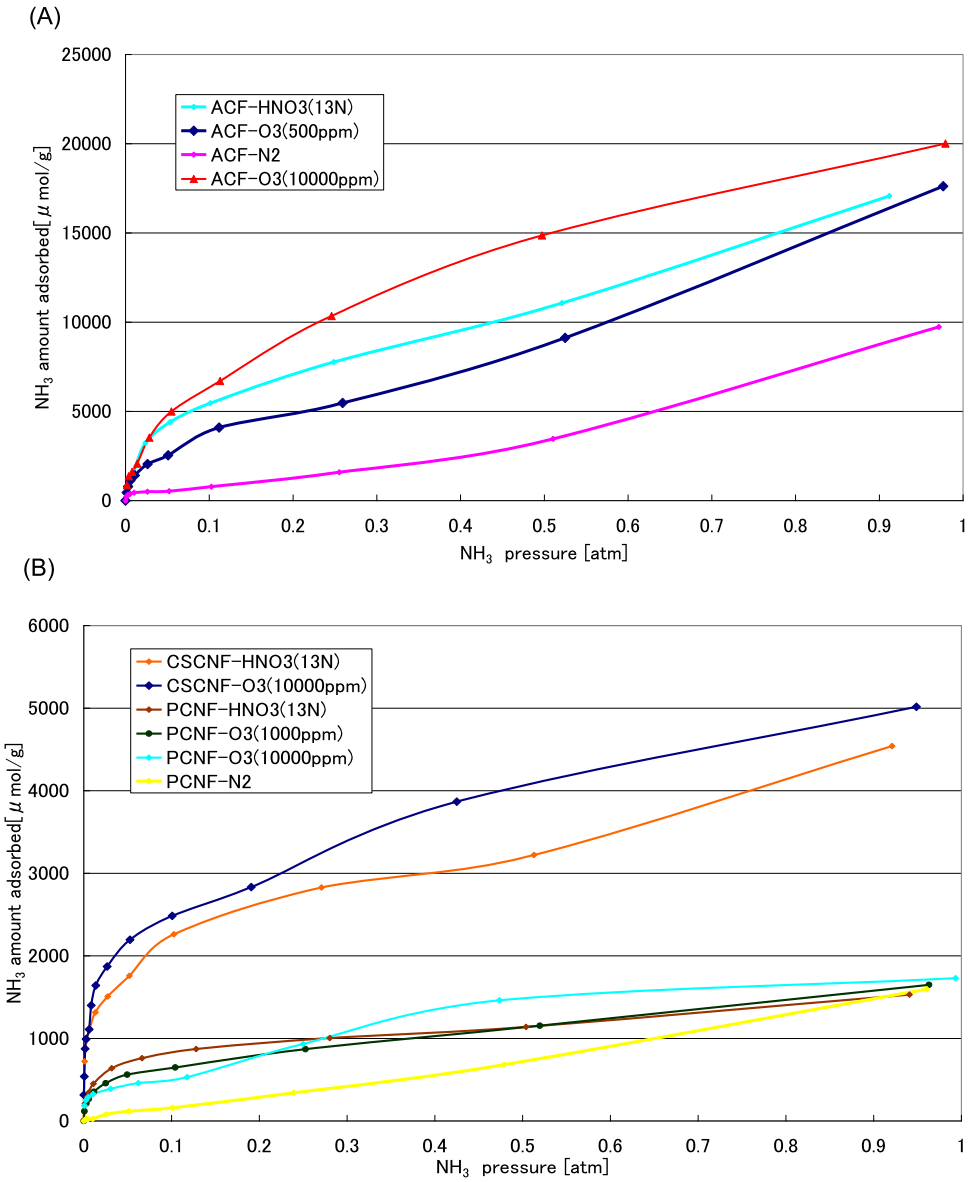

Fig. 9 Ammonia adsorption isotherm of PCNF, CSCNF and ACF before (**A**) and after (**B**) different oxidative treatments

3.4 Adsorption isotherms of ammonia and water

The ammonia adsorption isotherm results for the PCNF/CSCNF/ACF samples are shown in Fig. 9. All three samples showed enhanced ammonia adsorption with oxidization by ozone or nitric acid at low ammonia pressure ($p < 0.2$ atm). However, at relatively high ammonia pressure ($0.2 < p < 1$ atm), the amount of ammonia adsorbed on the PCNF–N_2 increased, as did those on the PCNF–O_3 and PCNF–HNO_3, indicating that the addition of oxygen-containing groups on the PCNF surface contributed to the increase in the NH_3 amount adsorbed only at the lower pressure range.

As shown in Fig. 9, in most of the isotherms the slope of the curves grew steep at around 0.2 atm, which may indicate a strong interaction between adsorbate molecules such as ammonia and water (Kaneko 1988; Kaneko et al. 1992; Furmaniak et al. 2005, 2008). These results indicate that the ammonia isotherms have different adsorption mechanisms in lower- and higher-pressure areas. We suggest that at the lower pressure range (0–0.2 atm), the most important cause of ammonia adsorption on PCNFs/CSCNFs/ACFs is the interaction between adsorbate and oxygen-containing functional groups on exposed edges, whereas at the higher pressure range (0.3–1.0 atm) the ammonia adsorption was derived from physisorption onto the carbon surface regardless of functional groups.

Our investigation of the effect of oxidization on each sample for ammonia adsorption confirmed that the initial amount adsorbed was enhanced by ozone or nitric acid treatment, and that the amount adsorbed on ACF–O_3 and ACF–HNO_3 were essentially the same, which is consistent with

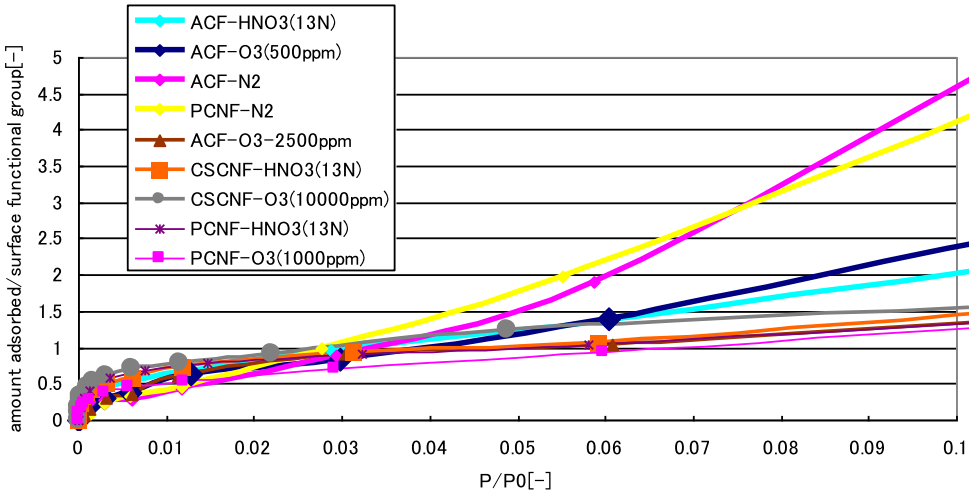

Fig. 10 The ratio of the amount of adsorbed ammonia to surface functional groups as a function of ammonia pressure

the results of our functional groups measurement by TPD analysis.

Since nitric acid oxidation broke the graphite structure of PCNFs/CSCNFs (as shown in Figs. 2, 3, 4), it was clarified that ozone treatment was better than nitric acid treatment, because the ozone treatment added CNF functional groups and ammonia adsorption capacity as well as the nitric acid treatment did, without destroying the graphite.

In addition, when we compared the oxidized samples, the amount adsorbed increased in the order of PCNF < CSCNF < ACF at 0–1 atm ammonia pressure. That order also corresponded to the result of the functional groups measurement by TPD analysis (Table 2). In addition, when we compared the ACF–N_2 and CSCNF–HNO_3, the CSCNF had a larger amount adsorbed than did the ACF at low pressure, but the amount adsorbed on ACF–N_2 exceeded that of CSCNF–O_3 at more than 0.5 atm. That is because CSCNF–HNO_3 had more oxygen-containing functional groups but a smaller surface area than ACF–N_2.

The ratios of ammonia amount adsorbed to total functional groups measured by TPD are shown in Fig. 10. The ratio of all samples corresponded to 1 at around $P/P_0 = 0.05$. Therefore, it could be said that at a lower pressure range ($P/P_0 < 0.05$) the adsorption phenomena were derived from one-to-one interaction between ammonia molecules and oxygen atoms of surface functional groups on PCNF/CSCNF/ACF, whereas at $P/P_0 > 0.05$ the ratio of ammonia amount adsorbed to total functional groups reached much more than 1 for ACF–N_2, PCNF–N_2, ACF–HNO_3 and ACF–O_3, which might be because adsorption on the carbon surface without oxygen-containing functional groups occurred. Actually, the fewer total functional groups per BET surface area the sample had, the higher its ratio of adsorbed amount to functional groups (Fig. 10). Thus, we conclude that in case of ACF–N_2, PCNF–N_2, ACF–HNO_3 and ACF–O_3, ammonia adsorption at relatively high pressure ($P/P_0 > 0.05$) was not related to the surface functional groups.

The results of the water adsorption isotherm for PCNF-O_3 and ACF-O_3 are shown in Figs. 11 and 13. Oxidization of PCNFs/ACFs improved the water adsorption performance at the lower pressure range ($P/P_0 = 0$–0.4) as well as ammonia adsorption, and thus the addition of surface oxygen-containing groups improved the adsorption performance of CNFs and ACFs for ammonia and water at the low pressure range. The PCNFs and ACFs showed curves similar to those reported in research concerning water adsorption on oxidized activated carbon (Salame and Bandosz 2002). It is noteworthy that the ratios of the amount of adsorbed water to functional groups for PCNF–O_3 and ACF–O_3 were the same value at $P/P_0 = 0$–0.4. This result indicates that the water adsorption on oxidized ACFs and PCNFs was based on the same adsorption mechanism depending not on porosity and surface area but on the interaction among water molecules or between water molecules and oxygen-containing functional groups. Salame and Bandosz (2002) also reported that the dominant factor in water adsorption on oxidized activated carbon was not porosity but the chemical functionality at the low pressure range. However, at high relative pressure, the ratio increased more sharply for PCNF–O_3, a result which might be derived from the unique functionality of CNFs, with densely added functional groups per BET surface area.

In addition, ammonia and water desorption from each PCNF and CSCNF sample was completed in less than 4 hr by vacuum at 298 K, which indicated that the adsorption phenomena in this study were reversible and that the adsorption energy was smaller than that of typical chemisorption between NH_3 and oxygen-containing functional groups.

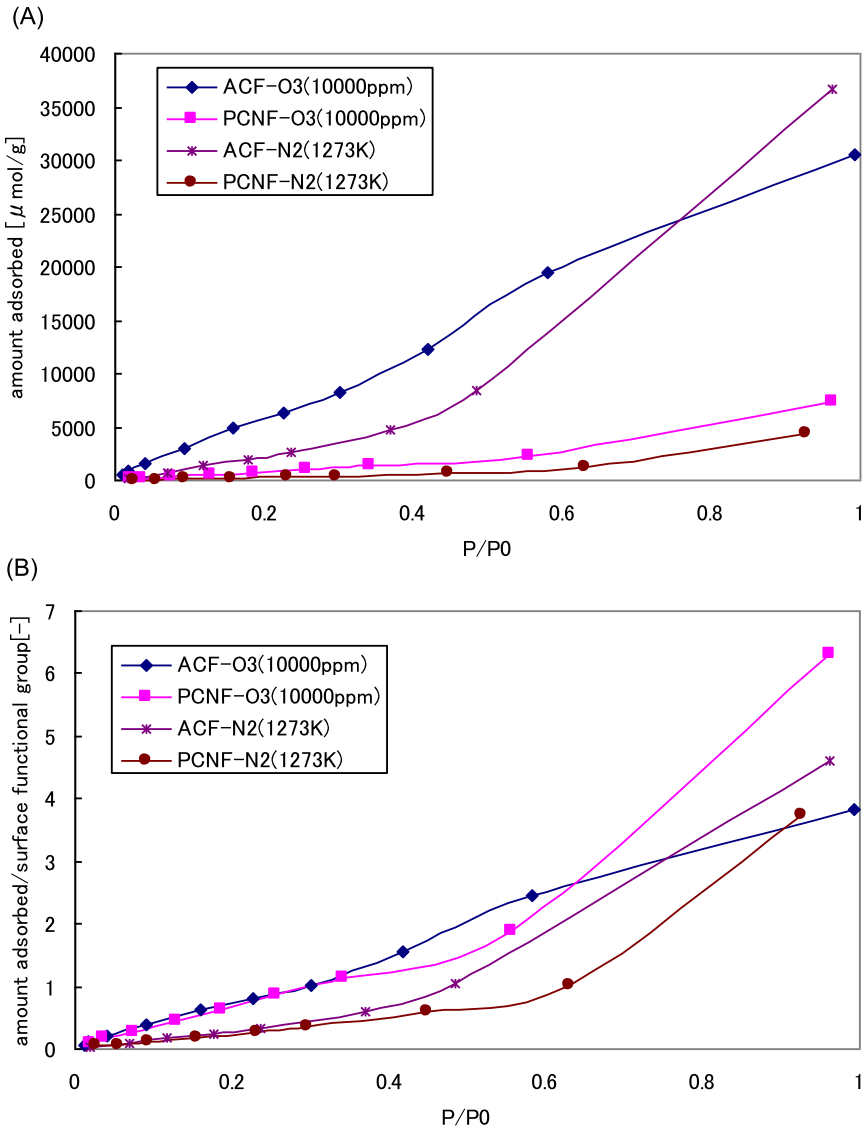

Fig. 11 (**A**) Water adsorption isotherm and (**B**) the ratio of the amount of adsorbed H_2O/NH_3 to surface functional groups as a function of gas pressure

3.5 Heat of adsorption of ammonia and water on functionalized PCNFs

To estimate the adsorption enthalpy change with ammonia and water adsorption on the surface of PCNFs and ACFs, we evaluated the isosteric heat of the adsorption of ammonia and water from adsorption isotherms (Figs. 12, 13) as follows:

$$\frac{d(\ln P)}{d(1/T)} = -\frac{q_{st}}{R} \tag{5}$$

where P is the adsorbate gas pressure, T is the temperature [K] and q_{st} is the isosteric heat of adsorption. Using Eq. (5), we calculated the $\ln P$ versus $1/T$ plots of ammonia and water adsorption isotherms from 300 to 323 K (Figs. 14A, 14B), and the q_{st} was evaluated from the slopes of the plots according to Eq. (5).

The dependencies of q_{st} on the amount adsorbed on PCNF–O_3 (10,000 ppm) and ACF–O_3 (10,000 ppm) are shown in Fig. 15A–15C.

At the initial stage of ammonia adsorption on PCNF–O_3, q_{st} was approx. 25 kJ/mol, and it then decreased to 10–12 kJ/mol with increased adsorption of NH_3, until the ratio of the amount adsorbed to total functional groups reached 1.4 (Fig. 15C). These q_{st} values were smaller than those of the enthalpy change of chemical adsorption, including acid-base reaction. For example, the enthalpy change of the reaction between carboxylic acid and basic groups was approx. 50 kJ/mol (The Chemical Society of Japan 1984). Our results mean that in the case of ammonia adsorption on PCNF–O_3, the ammonia molecule was adsorbed without strong interaction such as an acid-base reaction between ammonia and oxygen-containing groups.

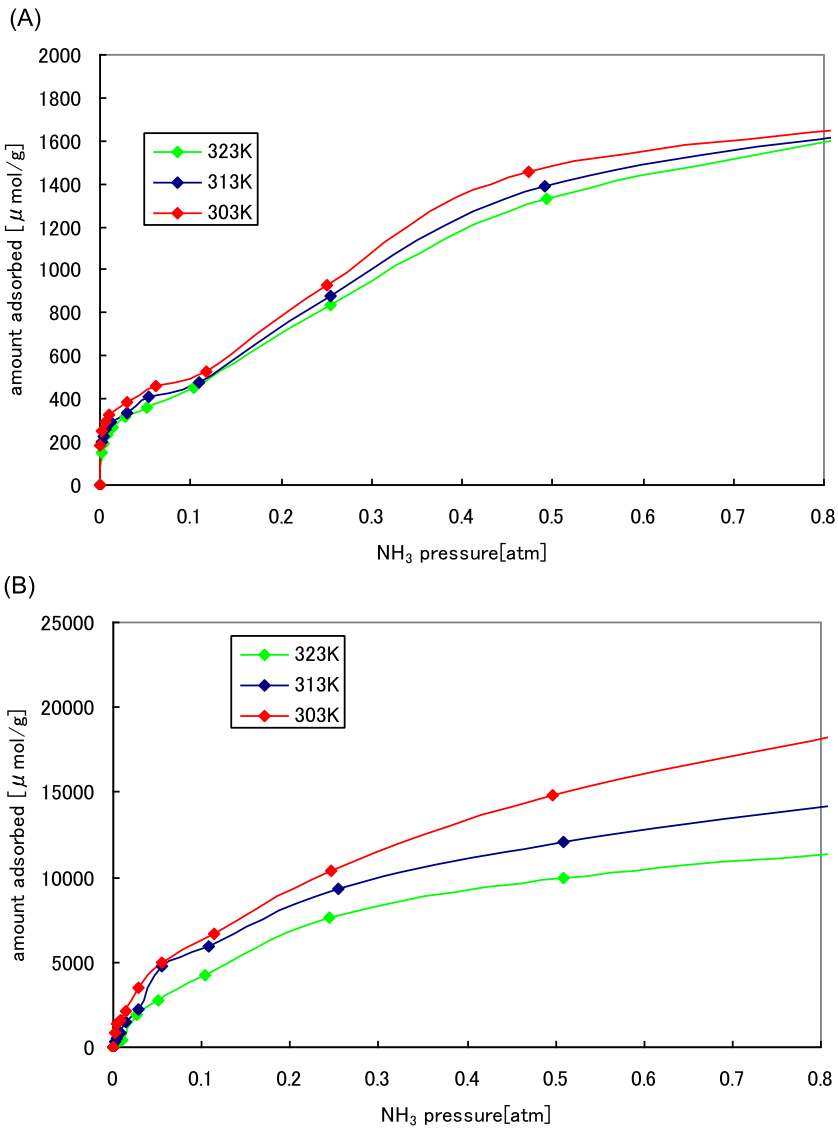

Fig. 12 Ammonia adsorption isotherm at 303, 313, 323 K on (**A**) PCNF–O_3 and (**B**) ACF–O_3

On the other hand, the initial adsorption heat of ammonia on ACF–O_3 was more than 100 kJ/mol, and it was always higher than that of PCNF–O_3, which might be because of the specific interaction via a Brønsted acid-base reaction between ammonia and oxygen-containing groups as well as a nonspecific interaction that is derived from the large surface area of ACFs and micropores (Bandosz and Petit 2009). In addition, a decrease in the isosteric heat of adsorption with gas loading like ACF–O_3 (Fig. 15A) is characteristic of highly heterogeneous adsorbents such as activated carbon with a wide distribution of gas-solid interaction energies (Thamm 1987; Dunne et al. 1996). These tendencies of ammonia adsorption on ACFs correspond to previous findings concerning the adsorption heat of ammonia on activated carbon (Xie et al. 2000) and some types of zeolite with an energetically heterogeneous surface (Zhang et al. 1990).

The above-mentioned experimental results and discussion suggest that the ammonia adsorption on functionalized PCNFs at the lower ammonia pressure range (0–0.2 atm) is not derived from a nonspecific interaction on the carbon surface or in micropores, or from a strong interaction via an acid-base reaction between adsorbate and oxygen-containing groups. We suggest that it occurred due to hydrogen bonds between ammonia and oxygen-containing groups.

Various studies of the strength of NH…O bonding energy indicated that the bonding is $\leq$ 30 kJ/mol. Since the bonding energy between NH_3 molecules and surface oxygen-containing groups by hydrogen bonding has been reported to be 12.6 kJ/mol (Lee and Reucroft 1999), it is likely that the ammonia adsorption heat on PCNF–O_3 consisted of the hydrogen bonding energy and/or interaction between ammonia molecules (10–30 kJ/mol) (Kikuta et al.

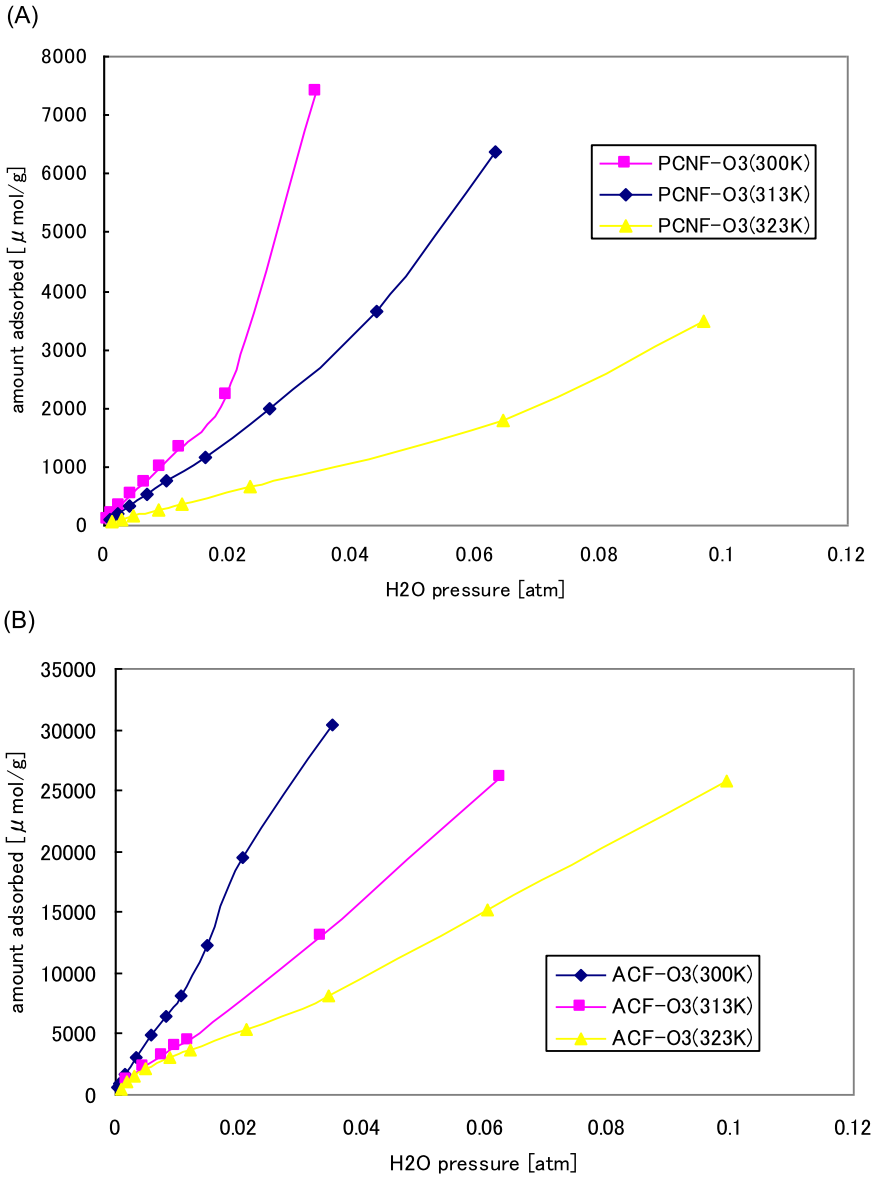

Fig. 13 Water adsorption isotherm at 30, 40, 50 °C on (**A**) PCNF–O_3 and (**B**) ACF–O_3

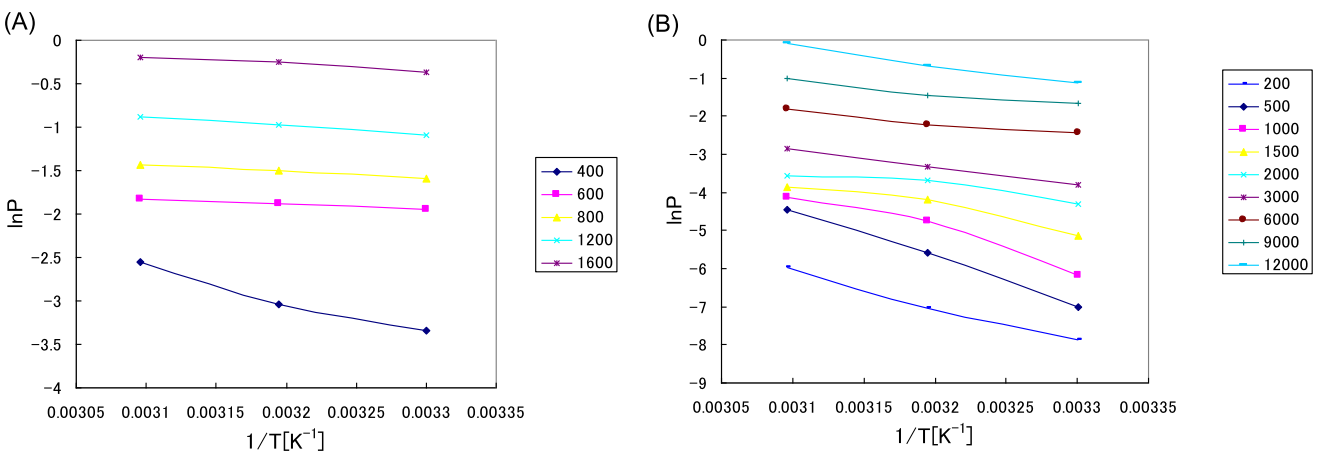

Fig. 14 ln P vs. $1/T$ plots of ammonia adsorption isotherms on (**A**) PCNF–O_3 and (**B**) ACF–O_3

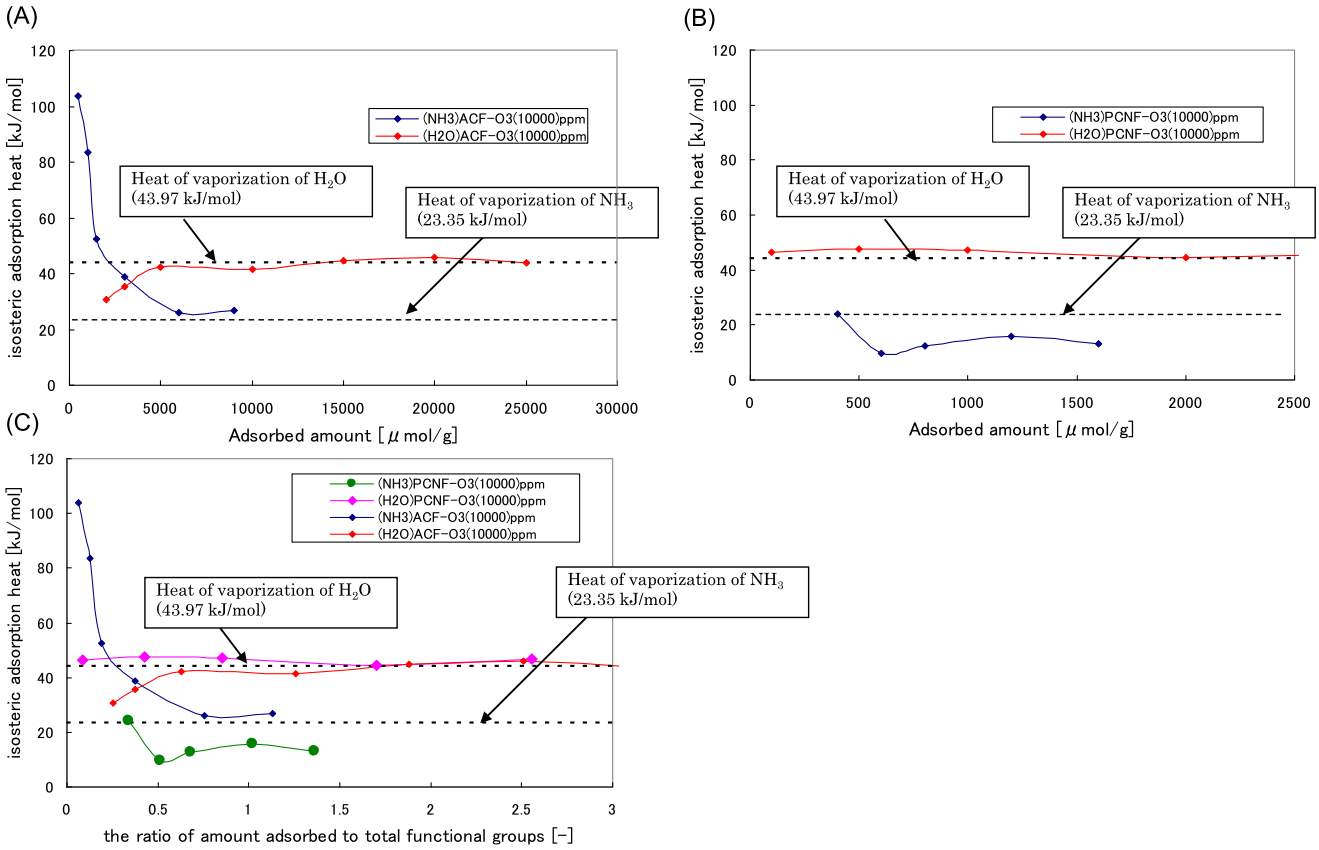

Fig. 15 Dependence of isosteric heat of adsorption of NH_3 and H_2O as a function of amounts adsorbed on (**A**) ACF-O3 and (**B**) PCNF-O_3; (**C**) indicates the dependence of heat of adsorption as a function of the ratio of the amount of adsorbed NH_3 and H_2O to surface functional groups

2008). In other studies, the interaction of NH…O bonding was evaluated as 10–13 kJ/mol in carbonylamine (Buemi and Zuccarello 2002), 11.3–16.3 kJ/mol in protein structure (Gilli et al. 2006), and 30.1 kJ/mol in N-methylacetamide dimer (Vargas et al. 2000). Thus, the interaction was ≤ 30 kJ/mol, and as such it is more likely that ammonia adsorption on the PCNFs in the present study was derived from hydrogen bonding rather than an acid-base reaction.

In the case of activated carbon, research groups investigating ammonia adsorption on oxidized activated carbon have reported the importance of chemical functionalities. For example, it was reported that ammonia molecules were adsorbed on oxidized activated carbon by a Brønsted acid-base reaction such as an ammonium salt generation reaction between ammonia and acid functional groups (Maruyama et al. 2003; Bandosz and Petit 2009). Similarly in the case of functionalized graphite oxide (GO), it was reported that ammonia molecule were adsorbed on GO by reactive adsorption forming amine or ammonium ions (Petit et al. 2009). Domingo-García et al. (2002) reported that ammonia was adsorbed on activated carbon through an irreversible reaction, but the phenolic groups had higher accessibility for ammonia molecules compared to that of the carboxylic groups, although the phenolic groups were less energetic than the carboxylic groups.

However, in a study by Xie et al. (2000), ammonia was adsorbed on oxidized activated carbon by weak bonding energy compared to an acid-base reaction such as the interaction between ammonia and carbonyl groups, which is likely to contain hydrogen bonding. In addition, in the case of ammonia adsorption on activated carbon functionalized by air oxidation, the interaction between adsorbate and activated carbon was not strong, and thus ammonia was completely desorbed by evacuation for 1 hr (Kaneko et al. 1992). Lee and Reucroft (1999) reported that ammonia adsorption on oxidized activated carbon was promoted by hydrogen bonding between ammonia molecules and surface functional groups, like the mechanism suggested in the present study. Thus, activated carbon could have an ammonia adsorption mechanism derived from a relatively weak hydrogen bond like the case of PCNFs. However, few authors have written about the quantitative relationship between the heat of adsorption and oxygen-containing groups or determined the specific mechanism of the adsorption, probably because the heat of adsorption on activated carbon was influenced mainly by a nonspecific interaction such as that with micropores on the carbon surface. We therefore examined ammo-

nia adsorption on PCNFs and ACFs to attempt to determine the mechanism derived from hydrogen bonding.

As shown in Figs. 15A–15C, the heat of the adsorption of water on PCNF–O_3 and ACF–O_3 produced almost the same plots at 44 kJ/mol, which corresponds to the vaporization heat of H_2O, indicating that water vapor adsorbed on an adsorbent surface has a condensed phase regardless of whether the surface is PCNFs or ACFs, except during the initial stage of adsorption. In this case, the heat of water adsorption on ACF–O_3 was smaller when the amount adsorbed was very small, as shown in Fig. 15A, and as the amount adsorbed increased, the heat of adsorption increased and remained at 44 kJ/mol when the ratio of the amount adsorbed to the total functional groups was approx. 0.7 (Fig. 15C).

These results may indicate that water molecules were adsorbed on ACF–O_3 by a relatively weak interaction between the water molecules and surface oxygen-containing groups at the initial stage of adsorption, and that when the amount adsorbed increased, the heat of the adsorption increased because hydrogen bonding between the water molecules increased, as in a previous study of water adsorption on activated carbon (Salame and Bandosz 2002). In contrast, the heat of water adsorption on PCNF–O_3 remained around at 44 kJ/mol throughout the water adsorption process. This result might be because the amount of total functional groups on PCNF–O_3 per BET surface area was large (as shown in Table 3), and then the water molecules adsorbed on oxygen-containing groups were easily interacted by hydrogen bonding since the distances between adsorbed water molecules were small.

This result supported our hypothesis stated in Sect. 3.4 that the water adsorption mechanism of PCNF–O_3 is consistent with that of ACF–O_3. Since past research has shown that the heat of water adsorption reached approx. 44 kJ/mol in the same way for activated carbon (Groszek and Aharoni 1999; Salame and Bandosz 2002) and graphite (CPC Society 1984), we conclude that this tendency is a common phenomenon in water vapor adsorption on a carbon surface, regardless of whether the surface is CNFs, ACFs, or graphite.

Since the heat of the ammonia adsorption on PCNF–O_3 was smaller than the heat of ammonia vaporization (23.35 kJ/mol), it is possible that ammonia molecules were adsorbed by a weak interaction between ammonia molecules, unlike the case with water adsorption. Earlier studies found that in the case of water or ammonia adsorption on graphite, the heat of adsorption showed the highest value at the initial stage and decreased with the increasing amount adsorbed to a minimum value that was lower than the heat of vaporization (Bomchil et al. 1979; CPC Society 1984). Therefore there is a possibility that PCNFs and graphite have the same characteristics in terms of the heat of adsorption because of their similar surface structure. In contrast, in the case of ammonia adsorption on ACF–O_3, the heat of adsorption was much larger than that of PCNF–O_3, probably because the interaction between ammonia molecules and the carbon surface or micropores was stronger than the interaction between the adsorbate and functional groups. In the present study, the heat of ammonia adsorption on ACF–O_3 was a steep downward-sloping curve, like that reported in a study of activated carbon without surface modification (Xie et al. 2000).

Our tests clarified that water adsorption mechanisms on oxidized PCNFs and ACFs were almost the same, based on their isotherms (Fig. 11) and heat of adsorption (Fig. 15), except in the high-pressure range. This heat of water adsorption result was due to the strong interaction among water molecules, regardless of the type of adsorbent. In the case of ammonia, the heat of adsorption was influenced by adsorbent characteristics such as the porosity of the ACFs.

As shown in Figs. 10 and 15, functionalized PCNFs and CSCNFs are likely to adsorb ammonia mainly by the interaction between functional groups and ammonia molecules, unlike ACFs, probably because their oxygen-containing groups are densely formed per BET surface area on their surface. However, it is likely that the adsorption mechanism of ammonia (i.e., the one-to-one interaction between functional groups and ammonia molecules and the heat of adsorption derived from hydrogen bonding) was the same for PCNFs and ACFs (and probably even for CSCNFs, because it has a structure similar to that of PCNFs, such as the abundant exposed edges and high density of surface functional groups per BET surface area).

4 Summary

Ammonia and water adsorption on oxidized PCNFs/CSCNFs were studied. Although their surface areas are smaller than that of ACFs, PCNFs/CSCNFs can support oxygen-containing groups in dense formation. Our results confirmed that the functionalization by ozone and nitric acid improved the ammonia adsorption amount on the PCNF/CSCNF surface. In particular, ozone treatment can add acid functional groups on PCNFs/CSCNFs without the graphite destructuring.

Our experimental results regarding NH_3 adsorption isotherms showed that the mechanism of ammonia adsorption on functionalized PCNFs at relatively low pressure is a one-to-one interaction between oxygen atoms in acid functional groups and hydrogen atoms in ammonia molecules, whereas the adsorption occurred mainly by interaction with the carbon surface at high pressure. When the ratios of the amount of ammonia adsorbed to functional groups were measured, they corresponded to 1 at the low relative pressure range ($P/P_0 = 0.04$–0.06).

In addition, the isosteric heat (q_{st}) of adsorption was calculated from the ammonia isotherm, which indicated that the

q_{st} of PCNF was derived from hydrogen bonding between NH…O and the interaction between ammonia molecules. Water adsorption on oxidized PCNFs and ACFs showed almost the same characteristics, depending on the strong interaction among water molecules, regardless of the type of adsorbent.

Acknowledgements Some of the experiments in this study were conducted at the Center for Nano Lithography and Analysis, The University of Tokyo, and were supported by the Ministry of Education, Culture, Sports, Science and Technology (MEXT, Japan). This work was partly supported by the Global COE Program, "The Physical Sciences Frontier" (MEXT, Japan), and also by an international cooperative program of the Japan Science and Technology Agency (JST, Japan).

References

Afuilar, C., García, R., Soto-Garrido, G., Arriagada, R.: Catalytic wet air oxidation of aqueous ammonia with activated carbon. Appl. Catal. B, Environ. **46**, 229–237 (2003)

Aksoylu, A.E., Madalena, M., Freitas, A., Fernando, M., Pereira, R., Figueiredo, J.L.: The effects of different activated carbon supports and support modifications on the properties of Pt/AC catalysts. Carbon **39**, 175–185 (2001)

Amorim, C., Yuan, G., Patterson, P.M., Keane, M.A.: Catalytic hydrodechlorination over pd supported on amorphous and structured carbon. J. Catal. **234**(2), 268–281 (2005)

Anderson, P.E.: A method for characterization and quantification of platelet graphite nanofiber edge crystal structure. Carbon **44**, 2184–2190 (2006)

Baker, R.T.K.: Catalytic growth of carbon filaments. Carbon **27**, 315–323 (1989)

Bandosz, T.J., Petit, C.: On the reactive adsorption of ammonia on activated carbons modified by impregnation with inorganic compounds. J. Colloid Interface Sci. **338**, 329–345 (2009)

Bessel, C.A., Laubernds, K., Rodriguez, N.M., Baker, R.T.K.: Graphite nanofibers as an electrode for fuel cell applications. J. Phys. Chem. B **105**(6), 1115–1118 (2001)

Bomchil, G., Harris, N., Leslie, M., Tabony, J., White, J.W., Gamlen, P.H., Thomas, R.K., Trewern, T.D.: Structure and dynamics of ammonia adsorbed on graphitized carbon black. Part 1. Adsorption isotherms and thermodynamic properties. J. Chem. Soc. Faraday Trans. I **1**(75), 1535–1541 (1979)

Buemi, G., Zuccarello, F.: Is the intramolecular hydrogen bond energy valuable from internal rotation barriers? J. Mol. Struct., Theochem **581**, 71–85 (2002)

Byl, O., Liu, J., Yates, J.T. Jr.: Etching of carbon nanotubes by ozone—a surface area study. Langmuir **21**, 4200–4204 (2005)

Chang, H., Lee, J.D., Lee, S.M., Lee, Y.H.: Adsorption of NH_3 and NO_2 molecules on carbon nanotubes. Appl. Phys. Lett. **79**(23), 3863–3865 (2001)

Chen, X., Xu, Z.H., Li, X., Shaibat, M.A., Ishii, Y., Ruoff, R.S.: Structural and mechanical characterization of platelet graphite nanofibers. Carbon **45**, 416–423 (2007)

CPC Society: Progress in Carbon Material Science II. Japan: Shigeji Hagiwara, pp. 55–64 (1984)

Delhaes, P., Couzi, M., Trinquecoste, M., Dentzer, J., Hamidou, H., Vix-Guterl, C.: A comparison between Raman spectroscopy and surface characterizations of multiwall carbon nanotubes. Carbon **44**, 3005–3013 (2006)

Domingo-García, M., Groszek, A.J., López-Garzón, F.J., Pérez-Mendoz, M.: Dynamic adsorption of ammonia on activated carbons measured by flow microcalorimetry. Appl. Catal. A, Gen. **233**, 141–150 (2002)

Dunne, J.A., Mariwala, R., Rao, M., Sircar, S., Gorte, R.J., Myers, A.L.: Calorimetric heats of adsorption and adsorption isotherms. 1. O_2, N_2, Ar, CO_2, CH_4, C_2H_6, and SF_6 on silicalite. Langmuir **12**, 5888–5895 (1996)

Endo, M., Hayashi, T., Kim, Y.A., Muramatsu, H.: Development and application of carbon nanotubes. J. Appl. Crystallogr. **45**, 4883–4892 (2006a)

Endo, M., Hayashi, T., Kim, Y.A., Muramatsu, H.: Nanocarbon. Filament and industry **60**(6), 260–265 (2006b) (in Japanese)

Feng, X., Irle, S., Witek, H., Morokuma, K., Vidic, R., Borguet, E.: Sensitivity of ammonia interaction with single-walled carbon nanotube bundles to the presence of defect sites and functionalities. J. Am. Chem. Soc. **127**, 10533–10538 (2005)

Figueiredo, J.L., Pereira, M.F.R., Freitas, M.M.A., Órfão, J.J.M.: Modification of the surface chemistry of activated carbons. Carbon **37**, 1379–1389 (1999)

Furmaniak, S., Terzyk, A.P., Gauden, P.A., Rychlicki, G.: Parameterization of the corrected Dubinin–Serpinsky adsorption isotherm equation. J. Colloid Interface Sci. **291**, 600–605 (2005)

Furmaniak, S., Gauden, P.A., Terzyk, A.P., Rychlicki, G.: Water adsorption on carbons—critical review of the most popular analytical approaches. Adv. Colloid Interface Sci. **137**, 82–143 (2008)

Gilli, P., Bertolasi, V., Pretto, L., Gilli, G.: Outline of a transition-state hydrogen-bond theory. J. Mol. Struct. **790**, 40–49 (2006)

Groszek, J.A., Aharoni, C.: Study of the active carbon−water interaction by flow adsorption microcalorimetry. Langmuir **15**, 5956–5960 (1999)

Guo, J., Xu, W.S., Chena, Y.L., Lua, A.C.: Adsorption of NH_3 onto activated carbon prepared from palm shells impregnated with H_2SO_4. J. Colloid Interface Sci. **281**, 285–290 (2005)

Hemraj-Benny, T., Bandosz, T.J., Wong, S.S.: Effect of ozonolysis on the pore structure, surface chemistry, and bundling of single-walled carbon nanotubes. J. Colloid Interface Sci. **317**, 375–382 (2008)

Huang, C.C., Li, H.S., Chen, C.H.: Effect of surface acidic oxides of activated carbon on adsorption of ammonia. J. Hazard. Mater. **159**, 523–527 (2008)

Kaneko, K.: Microporosity and adsorption characteristics against NO, SO_2, and NH_3 of pitch-based activated carbon fibers. Carbon **26**(3), 327–332 (1988)

Kaneko, K., Katori, T., Shimizu, K., Shindo, N., Maeda, T.: Changes in the molecular adsorption properties of pitch-based activated carbon fibres by air oxidation. J. Chem. Soc. Faraday Trans. **88**(9), 1305–1309 (1992)

Kikuta, Y., Ishimoto, T., Nagashima, U.: Deuterium-substituted water–ammonia mixed trimer clusters, $(H_2O)_n$—$3(NH_3)_n$ ($n = 0$, 1, 2, 3): interaction energy, hydrogen bond structures, and Mulliken population. Chem. Phys. **354**, 218–224 (2008)

Kim, S.D., Park, S.J., Lee, Y.S.: Chemical surface treatment for highly improved dispersibility of multi-walled carbon nanotubes in water. J. Dispers. Sci. Technol. **29**(3), 426–430 (2008)

Ko, S., Takahashi, Y., Fujita, H., Tatsuma, T., Sakoda, A., Komori, K.: Peroxidase-modified cup-stacked carbon nanofiber networks for electrochemical biosensing with adjustable dynamic range. RSC Adv. **2**, 1444–1449 (2012)

Kong, J., Franklin, N.R., Zhou, C., Chapline, M.G., Peng, S., Cho, K., Dai, H.: Nanotube molecular wires as chemical sensors. Science **287**, 622–625 (2000)

Lee, W.H., Reucroft, P.J.: Vapor adsorption on coal- and wood-based chemically activated carbons: (III) NH_3 and H_2S adsorption in the low relative pressure range. Carbon **37**, 21–26 (1999)

Lee, S., Kim, T.R., Ogale, A.A., Kim, M.S.: Surface and structure modification of carbon nanofibers. Synth. Met. **157**, 644–650 (2007)

Lu, J., Nagase, S., Maeda, Y., Wakahara, T., Nakahodo, T., Akasaka, T., Yu, D., Gao, Z., Han, R., Ye, H.: Adsorption configuration of NH_3 on single-wall carbon nanotubes. Chem. Phys. Lett. **405**, 90–92 (2005)

Marchon, B., Carrazz, J., Heinemann, H., Somorjai, G.A.: TPD and XPS studies of O_2 and CO_2, and H_2O adsorption on clean polycrystalline graphite. Carbon **26**, 507–514 (1988)

Maruyama, K., Takada, H., Kodama, M., Hatori, H., Yamada, Y., Asakura, R., Izumida, H., Morita, M.: Ammonia adsorption on porous carbons with acidic functional groups. Tanso **208**, 109–113 (2003)

Melechko, A.V., Merkulov, V.I., McKnight, T.E., et al.: Vertically aligned carbon nanofibers and related structures: controlled synthesis and directed assembly. J. Appl. Phys. **97**(4), 041301 (2005)

Niimi, Y., Matsui, T., Kambara, H., Tagami, K., Tsukada, M., Fukuyama, H.: Scanning tunneling microscopy and spectroscopy studies of graphite edges. Appl. Surf. Sci. **241**, 43–48 (2005)

Park, S.J., Kim, K.D.: Adsorption behaviors of CO_2 and NH_3 on chemically surface-treated activated carbons. J. Colloid Interface Sci. **212**, 186–189 (1999)

Park, S.J., Jin, S.Y.: Effect of ozone treatment on ammonia removal of activated carbons. J. Colloid Interface Sci. **286**, 417–419 (2005)

Peng, N., Zhang, Q., Chow, C.L., Tan, O.K., Marzari, N.: Sensing mechanisms for carbon nanotube based NH_3 gas detection. Nano Lett. **9**(4), 1626–1630 (2009)

Petit, C., Seredych, M., Bandosz, T.J.: Revisiting the chemistry of graphite oxides and its effect on ammonia adsorption. J. Mater. Chem. **19**, 9176–9185 (2009)

Ren, X., Chen, C., Nagatsu, M., Wang, X.: Carbon nanotubes as adsorbents in environmental pollution management: a review. Chem. Eng. J. **170**(2–3), 395–410 (2011)

Rivera-Utrilla, J., Sánchez-Polo, M., Gómez-Serrano, V., Álvarez, P.M., Alvim-Ferraz, M.C., Dias, J.M.: Activated carbon modifications to enhance its water treatment applications. An overview. J. Hazard. Mater. **187**, 1–23 (2011)

Rosenthal, D., Ruta, M., Schlögl, R., Kiwi-Minsker, L.: Combined XPS and TPD study of oxygen-functionalized carbon nanofibers grown on sintered metal fibers. Carbon **48**, 1835–1843 (2010)

Salame, I.I., Bandosz, T.J.: Interactions of water, methanol and diethyl ether molecules with the surface of oxidized activated carbon. Mol. Phys. **100**(13), 2041–2048 (2002)

Shan, X., Zhu, S., Zhang, W.: Effect of surface modification of activated carbon on its adsorption capacity for NH_3. J. China Univ. Mining & Technol. **18**, 0261–0265 (2008)

Shirvani, B.B., Beheshtian, J., Esrafili, M.D., Hadipour, N.L.: DFT study of NH_3 adsorption on the (5,0), (8,0), (5,5) and (6,6) single-walled carbon nanotubes. Calculated binding energies, nmR and NQR parameters. Physica B: Condens. Matter **405**, 1455–1460 (2010)

Sinha, N., Ma, J., Yeow, J.T.W.: Carbon nanotube-based sensors. J. Nanosci. Nanotechnol. **6**, 573–590 (2006)

Takahashi, Y., Fujita, H., Lin, W.H., Li, Y.Y., Fujii, T., Sakoda, A.: Synthesis of carbon nanofibers from poly(ethylene glycol) with controlled structure. Adsorption **16**, 57–68 (2010)

Tamon, H., Okazaki, M.: Influence of acidic surface oxides of activated carbon on gas adsorption characteristics. Carbon **34**, 741–746 (1996)

Thamm, H.: Adsorption site heterogeneity in silicalite: a calorimetric study. Zeolites **7**, 341–346 (1987)

The Chemical Society of Japan: Chemistry-Handbook (basic edition), 3rd ed., Japan (1984)

Tibbetts, G.G., Lake, M.L., Strong, K.L., et al.: A review of the fabrication and properties of vapor-grown carbon nanofiber/polymer composites. Compos. Sci. Technol. **67**(7–8), 1709–1718 (2007)

Vargas, R., Garza, J., Dixon, D.A., Hay, B.P.: How strong is the C^{α}–H...O=C hydrogen bond? J. Am. Chem. Soc. **122**, 4750–4755 (2000)

Wang, J.: Carbon-nanotube based electrochemical biosensors: a review. Electroanalysis **17**(1), 7–14 (2005)

Wang, Y., Wu, J., Wei, F.: A treatment method to give separated multi-walled carbon nanotubes with high purity, high crystallization and a large aspect ratio. Carbon **41**, 2939–2948 (2003)

Wu, L., Zhang, X., Ju, H.: Amperometric glucose sensor based on catalytic reduction of dissolved oxygen at soluble carbon nanofiber. Biosens. Bioelectron. **23**, 479–484 (2007)

Xie, F., Phillips, J., Silva, I.F., Palma, M.C., Menendez, J.A.: Microcalorimetric study of acid sites on ammonia- and acid-pretreated activated carbon. Carbon **38**, 691–700 (2000)

Yanagisawa, T., Hayashi, T., Kim, Y.A., Fukai, Y., Endo, M.: Structure and basic properties of cup-stacked type carbon nanofiber. Mol. Cryst. Liq. Cryst. **387**, [391]167–[395]171 (2002)

Yang, K., Han, H., Pan, X., Chen, N., Gu, M.: The effect of chemical treatment on the crystallinity of multi-walled carbon nanotubes. J. Phys. Chem. Solids **69**, 222–229 (2008)

Yoon, S.H., Lim, S., Hong, S.H., Mochida, I., An, B., Yokogawa, K.: Carbon nano-rod as a structural unit of carbon nanofibers. Carbon **42**, 3087–3095 (2004)

Zhang, D., Du, C., He, M., Min, E.: Characterisation of heterogeneous catalysts by modified flow microcalorimetry. Thermochim. Acta **165**, 171–182 (1990)

Zhang, S.J., Yu, H.Q., Feng, H.M.: PVA-based activated carbon fibers with lotus root-like axially porous structure. Carbon **44**, 2059–2068 (2006)

Zhao, N., Wei, N., Li, J., Qiao, Z., Cui, J., He, F.: Surface properties of chemically modified activated carbons for adsorption rate of Cr (VI). Chem. Eng. J. **115**, 133–138 (2005)

Zhuang, Q.L., Kyotani, T., Tomita, A.: DRIFT and TK/TPD analyses of surface oxygen complexes formed during carbon gasification. Energy Fuels **8**(3), 714–718 (1994a)

Zhuang, Q.L., Kyotani, T., Tomita, A.: The change of TPD pattern of O_2-gasified carbon upon air exposure. Carbon **32**, 539–540 (1994b)